Journal of Microbiology (2015) Vol. 53, No. 10, pp. 711–717
DOI 10.1007/s12275-015-5417-5


# Structural basis for the ATP-independent proteolytic activity of LonB proteases and reclassification of their AAA+ modules[§]

**Young Jun An[1†], Jung-Hyun Na[1†], Myung-Il Kim[1†], and Sun-Shin Cha[1,2,3*]**

[1]*Marine Biotechnology Research Center, Korea Institute of Ocean Science and Technology, Ansan 15627, Republic of Korea*
[2]*Department of Marine Biotechnology, Korea University of Science and Technology, Daejeon 34113, Republic of Korea*
[3]*Department of Convergence Study on the Ocean Science and Technology, Ocean Science and Technology School, Korea Maritime and Ocean University, Pusan 49112, Republic of Korea*

(Received Aug 20, 2015 / Revised Sep 14, 2015 / Accepted Sep 14, 2015)

**Lon proteases degrade defective or denature proteins as well as some folded proteins for the control of cellular protein quality. There are two types of Lon proteases, LonA and LonB. Each consists of two functional components: a protease component and an ATPase associated with various cellular activities (AAA+ module). Here, we report the 2.03 Å-resolution crystal structure of the isolated AAA+ module (*i*AAA+ module) of LonB from *Thermococcus onnurineus* NA1 (*Ton*LonB). The *i*AAA+ module, having no bound nucleotide, adopts a conformation virtually identical to the ADP-bound conformation of AAA+ modules in the hexameric structure of *Ton*LonB; this provides insights into the ATP-independent proteolytic activity observed in a LonB protease. Structural comparison of AAA+ modules between LonA and LonB revealed that the AAA+ modules of Lon proteases are separated into two distinct clades depending on their structural features. The AAA+ module of LonB belongs to the 'H2 & Ins1 insert clade (HINS clade)' defined for the first time in this study, while the AAA+ module of LonA is a member of the HCLR clade.**

***Keywords***: AAA+ proteins, PS-1 insert, H2 insert, Ins1, Lon proteases, *Thermococcus onnurineus* NA1, ATP-independent proteolytic activity

## Introduction

ATP-dependent proteases play important roles in cellular protein quality control and homeostasis as well as regulation of many cellular processes by selectively degrading regulatory proteins (Goldberg and St John, 1976; Hershko and Ciechanover, 1992; Gottesman, 2003; Sauer *et al.*, 2004; McClellan *et al.*, 2005; Talarico *et al.*, 2005). In prokaryotic cells and in the organelles of higher eukaryotes, energy-dependent proteolysis is accomplished by oligomeric ATP-dependent proteases, such as Lon, FtsH, ClpAP, ClpXP, and HslUV (Gottesman, 1996). Each consists of two functional parts: a protease component, assembled into barrel-shaped complexes with an internal chamber in which the proteolytic sites are sequestered, and an oligomeric ring-shaped ATPase associated with various cellular activities (AAA+ module). Substrate proteins are recognized by the AAA+ ring, either directly or via adaptor proteins. ATP binding/hydrolysis cycles drive conformational changes of the AAA+ ring that create mechanical forces that denature substrates and translocate them into the proteolytic sites (Sauer and Baker, 2011). Lon and FtsH contrast with ClpAP, ClpXP, and HslUV, which are assembled from an independently expressed AAA+ component and a protease component, since AAA+ and protease components of Lon and FtsH exist in a single polypeptide.

Lon is the first identified ATP-dependent protease whose orthologues are found in all kingdoms of life including human being. Emerging evidence suggests that Lon proteases are divided into two subgroups, LonA and LonB. LonA, found in all bacteria and in eukaryotic cell organelles, and LonB, found only in Archea, are different in their domain compositions. LonA is composed of an N-terminal domain (LAN), an AAA+ domain, and a protease domain, whereas LonB consists of a protease domain and an AAA+ domain containing a membrane-spanning region that anchors the protein in the cytoplasmic surface of the membrane (Rotanova *et al.*, 2006). Here, we report the crystal structure of the isolated AAA+ module (*i*AAA+ module) of LonB from *Thermococcus onnurineus* NA1 (*Ton*LonB) with the membrane-spanning region deleted. The limited proteolysis of the hexameric *Ton*LonB by trypsin gave rise to the *i*AAA+ module. Structural comparison of the *i*AAA+ module with AAA+ modules in the hexameric *Ton*LonB structure (Cha *et al.*, 2010) suggests that mechanical forces could be generated even in the absence of ATP. In addition, the structure of the *i*AAA+ module discriminated from the AAA+ module of a LonA protease reveals that the AAA+ modules of Lon proteases are separated into two distinct clades depending on their structural features.

## Materials and Methods

### Expression, purification, and crystallization

*Ton*LonB was expressed and purified as previously described

[†]These authors contributed equally to this work.
*For correspondence. E-mail: chajung@kiost.ac.kr; Tel.: +82-31-400-6297; Fax: +82-31-406-6297
[§]Supplemental material for this article may be found at http://www.springerlink.com/content/120956.

**Table 1. Data collection and refinement**

| | |
|---|---|
| Data collection | |
| Space group | *P*1 |
| Wavelength (Å) | 1.00000 |
| Cell dimensions | |
| *a*, *b*, *c* (Å) | 40.620, 61.599, 76.321 |
| α, β, γ (deg) | 74.607, 87.110, 83.451 |
| Resolution (Å) [a] | 50-2.03 |
| Total No. of reflections | 230492 |
| No. of unique reflections | 42270 |
| Completeness (%)[a] | 93.1 (82.6) |
| $R_{sym}$ (%)[a,b] | 4.2 (20.9) |
| $I/\sigma$ (*I*) [a] | 23.03 (3.09) |
| Redundancy | 2.3 (1.8) |
| Refinement statistics | |
| Resolution range (Å) | 41.14-2.03 |
| No. reflections | 40140 |
| No. atoms | |
| Protein | 4960 |
| Water | 243 |
| Glycerol | 6 |
| *B*-factors | |
| Protein | 34.07 |
| Water | 37.04 |
| Glycerol | 44.59 |
| $R_{work}$ / $R_{free}$ (%)[c] | 18.2 (23.9) |
| r.m.s. deviations[d] | |
| Bonds length (Å) | 0.018 |
| Bond Angles (°) | 1.856 |

[a]The number in parentheses is for the outer shell.
[b]$R_{sym} = \Sigma_h\Sigma_I |I_{h,i}-I_h| / \Sigma_h\Sigma_I\Sigma\Sigma I_{h,i}$, where $I_h$ is the mean intensity of the i observations of symmetry related reflections of h.
[c]$R_{work} = \Sigma |F_o-F_c| / \Sigma F_o$, where $F_o = F_p$, and $F_c$ is the calculated protein structure factor from the atomic model. $R_{free}$ was calculated with 5% of the reflections.
[d]r.m.s. deviations in bond length and angles are the deviations from ideal values.

(An *et al.*, 2010). Briefly, the *Ton*LonB gene, with deletion of a membrane-anchoring region (residues 134-170), was cloned into pET24a (Novagen). The expression vector was transformed into *Escherichia coli* BL21(DE3) (Stratagene). The transformed cells were grown in Luria–Bertani medium (Merck) containing 50 μg/ml kanamycin to an $OD_{600}$ of 0.5 at 310 K, and the expression of *Ton*LonB was induced with 1 mM isopropyl-1-thio-β-D-galactopyranoside (Duchefa). After 7 h induction at 303 K, cells were harvested and resuspended in 10 mM Tris-HCl (pH 7.5). The cells were disrupted by sonication and the crude lysate was centrifuged at 20,000 × *g* for 60 min at 277 K. The resulting supernatant was loaded into a nickel-nitrilotriacetic acid column (Qiagen). The column was washed with a washing buffer containing 10 mM Tris-HCl (pH 7.5) and 20 mM imidazole. *Ton*LonB was eluted with the same buffer containing 300 mM imidazole. The eluted fraction was loaded on a Q-Sepharose Fast Flow column (Qiagen) and eluted with a 0–1 M NaCl gradient in 10 mM Tris (pH 7.5) containing 1 mM DTT.

To isolate the AAA+ module, limited proteolysis was carried out by incubating the full length *Ton*LonB with trypsin (1:100 w/w) for 50 min at 353 K, and the mixture was loaded onto Superdex S75 prep grad (GE Health) with buffer containing 10 mM Tris-HCl (pH 7.5), 100 mM NaCl, and 1 mM DTT. The fractions, including the AAA+ module, were collected and concentrated to ~12 mg/ml for crystallization.

The batch crystallization method was used for crystal screening and optimization at 295 K. Small drops composed of 1 μl protein solution and an equal volume of crystallization reagent were pipetted under a layer of a 1:1 mixture of Silicon oil and Paraffin oil in 72-well HLA plates (NUNC). Crystal screening was performed with all the available screening kits from Hampton Research and Emerald BioSystems. Initial crystals of *i*AAA+ module of *Ton*LonB were grown in a precipitant containing 0.2 M potassium chloride, 0.01 M magnesium acetate, 0.05 M tri-sodium citrate dihydrate pH 4.5, and 12% PEG 4000 (condition No. 23 of Natrix Screen from Hampton Research). The crystallization condition was then optimized to 0.2 M potassium chloride, 0.01 M magnesium acetate, 0.05 M tri-sodium citrate dihydrate pH 4.5, 12% PEG 4000, and 5% w/v n-Dodecyl-β-d-maltoside.

### Data collection and refinement

For data collection at 100 K, a crystal was transferred to a cryoprotectant solution containing 20% glycerol in the same mother liquor. A 2.03-Å dataset was collected at beamline 17A at the Photon factory, Japan (Table 1). The data was integrated and scaled with HKL2000 (Otwinowski and Minor, 1997). The crystal belonged to a space group, *P*1, with two monomers per asymmetric unit and unit cell dimensions of *a*=40.6 Å, *b*=61.6 Å, *c*=76.3 Å, α=74.6°, β=87.1°, and γ=83.5°. The structure of the *i*AAA+ module was determined by molecular replacement with MolRep in the *CCP4* program suite (Collaborative Computational Project, 1994). The structure of the AAA+ module in the hexameric *Ton*LonB was exploited as a search model (Cha *et al.*, 2010). Manual model building and refinement (Table 1) were performed by using Coot (Emsley and Cowtan, 2004) and PHENIX (Adams *et al.*, 2002), respectively. The Ramachandran plot of the final model with *R* and $R_{free}$ values of 18.2% and 23.9%, respectively, indicates that 96.7% of non-glycine residues are in the most favored regions and that the remaining 2.9% residues are in the allowed region. Structure comparison and analyses were carried out by using the program Superimpose in the *CCP4* program suite (Collaborative Computational Project, 1994), and figures were prepared by using PyMOL (The PyMOL Molecular Graphics System, Version 1.7.4, Schrödinger, LLC.).

### Data deposition

Atomic coordinates and structure factors have been deposited in the Protein Data Bank (PDB; accession code 4ZPX).

## Results and Discussion

### Crystal structure of the *i*AAA+ module in *Ton*LonB

The 412-residue *i*AAA+ module of *Ton*LonB has a modular structure composed of three subdomains; a α/β-subdomain, a α-subdomain, and a portal subdomain (Fig. 1A). The α/β-subdomain (residues 39–323) adopts the typical RecA-fold with a central five-stranded parallel β-sheet (β12-, β1-, β11-, β8-, and β5, in order) sandwiched by six α-helices

(α3, α4, α6, α8, α10, and α13) and three $3_{10}$ helices (α2, α9, and α12). The α-subdomain (residues 324–412) is composed of a four-helix bundle (α14, α15, α16, and α17), a two-stranded antiparallel β-strand (β13 and β14), and a $3_{10}$ helix (α1). The N-terminal residues (20–38) extensively interact with the α-helical subdomain.

The ATP-binding site is situated at the interface between the α/β-subdomain and the α-subdomain (Cha *et al.*, 2010). Motifs for ATP hydrolysis and nucleotide sensing are well conserved at the interface. The α/β-subdomain has three highly conserved motifs: Walker-A (residues 67–74), which interacts with the β and γ phosphates of ATP; Walker-B (residues 241–246), which activates a water molecule that attacks the β-γ phosphodiester bond of ATP, and sensor-1 (residues 297–300), which communicates with the γ-phosphate and is used to discriminate between ATP and ADP (Figs. 1A and 2). The α-helical subdomain contains the sensor-2 motif (Figs. 1A and 2), which is also used to discriminate among nucleotide states. Despite the conservation of functional motifs, the *i*AAA+ module has no ATPase activity. In the hexameric conformation, an arginine finger (Arg311) in one AAA+ module stabilizes negative charge of γ phosphate of ATP bound to the adjacent AAA+ module, which is essential for ATP hydrolysis (Cha *et al.*, 2010). The *i*AAA+ module exists as a monomer due to the absence of the protease domain, which indicates that the arginine finger cannot be provided by an adjacent AAA+ module.

The portal subdomain is composed of three insertions emerging from the α/β-subdomain: insertion 1 (Ins1; residues 85–189), insertion 2 (Ins2; residues 209–232), and insertion 3 (Ins3; residues 266–288) (Fig. 2). Ins1, lying between helix 4 (α4) and strand 5 (β5), adopts a simple α/β fold with a three-stranded antiparallel β-sheet packed with one helix. Ins1 includes an unstructured or mobile substructure surrounding the membrane-anchoring region not visible in our structure (Fig. 1A). Ins2 (located between α6 and α8) and Ins3 (connects α10 and β11) are commonly comprised of two antiparallel β-strands connected by a $3_{10}$ helix (Fig. 1A). The three inserts interact extensively with each other. Ile92, Val94, Pro104, Ile106, and Leu185 in Ins1; Val211 and Val229 in Ins2; and Ile269, Thr283, and Val286 in Ins3 constitute a hydrophobic core (Fig. 1A and B). In the active hexameric conformation of *Ton*LonB (Fig. 1C), a hexagonal cylinder with a large sequestered chamber accessible through an axial channel and six portal subdomains form a pore that plays a role as a gated portal for substrate entry (Cha *et al.*, 2010).

## Structural basis for the ATP-independent proteolytic activity

We have previously reported that the AAA+ modules of *Ton*LonB adopt two distinct conformational states in the active hexameric structure (Cha *et al.*, 2010). The L- and T-states are observed in the AAA+ modules with a loosely-bound ADP (L-AAA+ module) and a tightly-bound ADP (T-AAA+ module), respectively (Cha *et al.*, 2010). Therefore, L- and T-states are thought to represent conformational

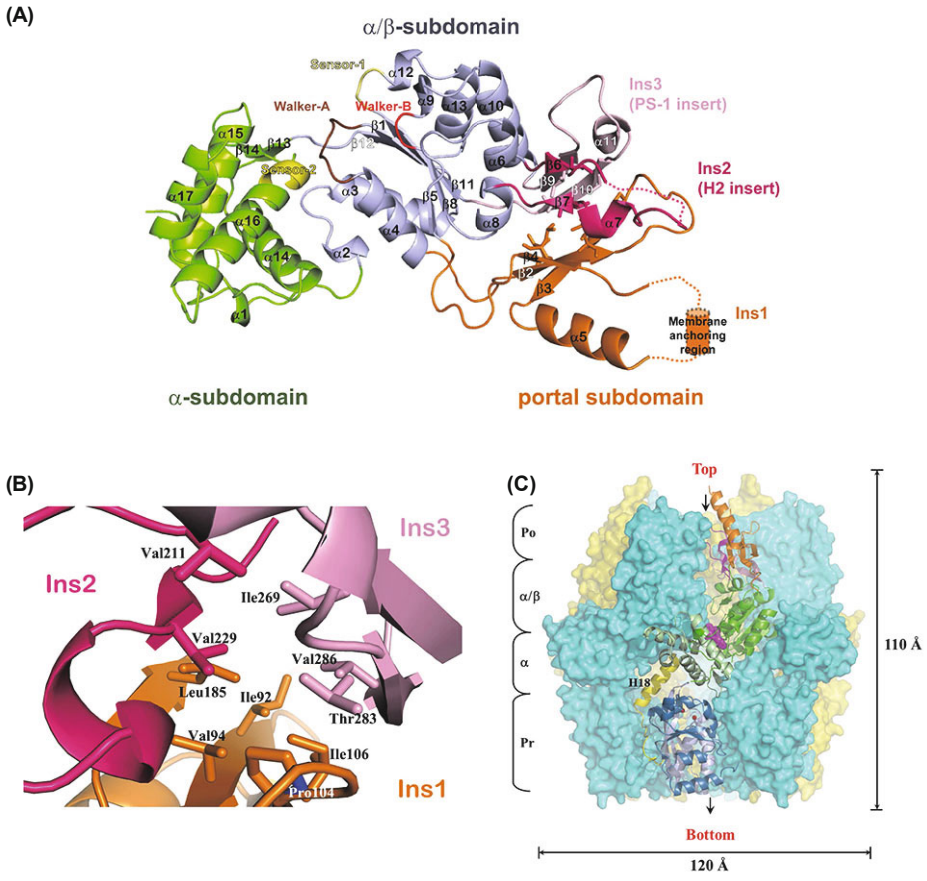


**Fig. 1. The overall structure of the *i*AAA+ module.** Ins1, Ins2 (H2 insert), and Ins3 (PS-1 insert) are highlighted in orange, hot pink, and light pink, respectively. (A) Ribbon diagram of the *i*AAA+ module. The α-subdomain, α/β-subdomain, Walker-A, Walker-B, sensor-1, and sensor-2 are shown in green, light blue, brown, red, light yellow, and yellow, respectively. α-Helices and β-strands are numbered consecutively from the N-terminus to the C-terminus. Putative membrane-anchoring region and disordered region of H2-insert are presented by dotted line. (B) Close-up view of the portal subdomain. Ten residues (Ile92, Val94, Pro104, Ile106, and Leu185 in Ins1; Val211 and Val229 in Ins2; Ile269, Thr283, and Val286 in Ins3) constituting the hydrophobic core are shown in sticks. (C) The hexameric structure of *Ton*LonB (Cha *et al.*, 2010). The hexamer is shown with five subunits in surface representation and one monomer as a ribbon diagram. The molecule is oriented with the protease domain (Pr) (blue and light blue ribbons) at the bottom, the α-subdomain (α) (light green ribbon) in the middle, and the α/β-subdomain (α/β) (green ribbon) with portal subdomain (Po) (orange, magenta, and light pink ribbons) at the top. ADP is represented as a stick with surface representation between the α/β and the α-subdomains. L- and T-monomers are colored in cyan and yellow, respectively. The monomer shown by a ribbon diagram is in T-state.

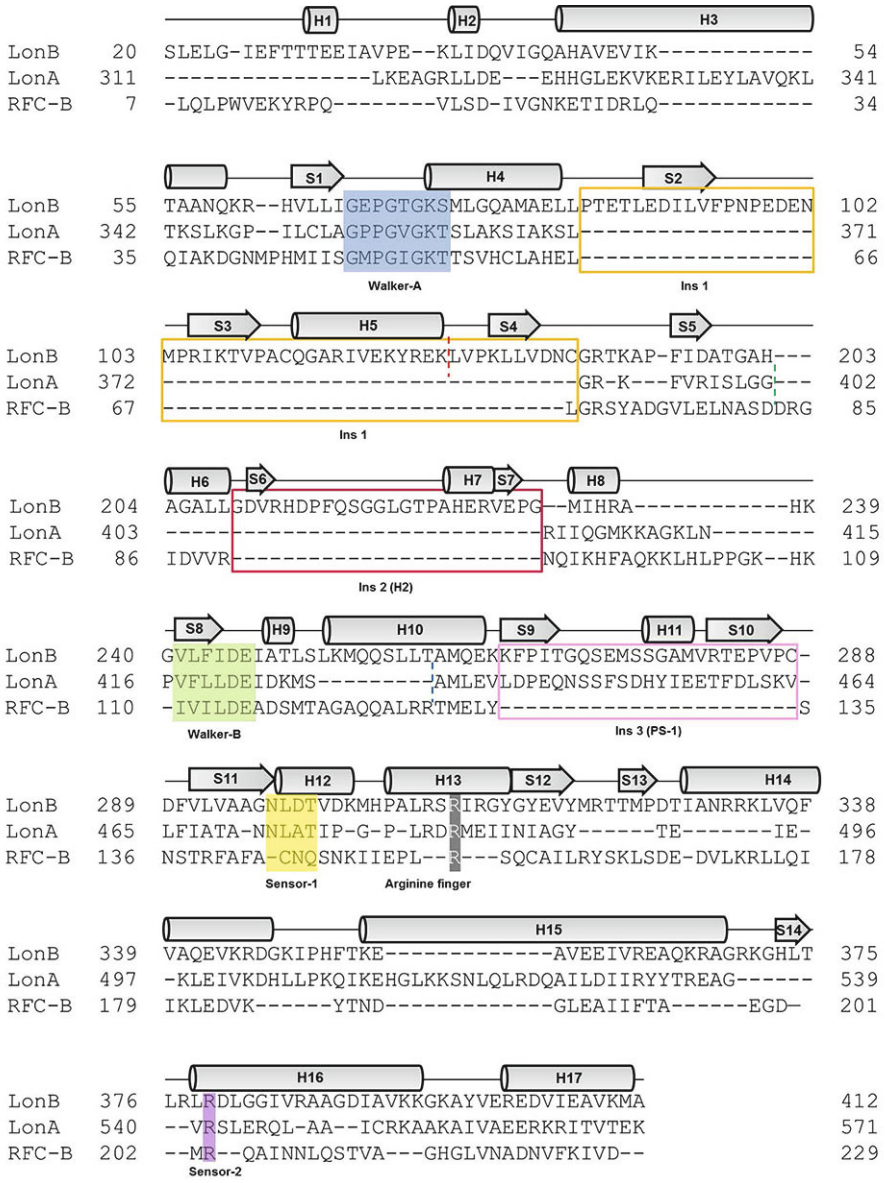


**Fig. 2. Sequence alignment of the AAA+ modules of RFC-B, *Bs*LonA, and *Ton*LonB.** Residues 134–170 corresponding to the putative membrane-anchoring region within Ins1 (an orange box) of LonB are not shown. Residues 382–402 and 427–436 corresponding to the disordered region in the structure of *Bs*LonA (PDB code 3M6A) are also not shown. Red, green, and blue dotted vertical lines indicate the position of residues 134–170 (*Ton*LonB), 382–402 (*Bs*LonA), and 427–436 (*Bs*LonA), respectively. Ins2 and Ins3 are boxed in hot pink and light pink, respectively. Walker-A, Walker-B, sensor-1, sensor-2, and arginine finger residues are shaded blue, green, yellow, purple, and gray, respectively. The secondary structure assignment corresponds to *i*AAA+ module of *Ton*LonB.

states before ATP binding and after ATP hydrolysis, respectively. It is likely that the AAA+ module of *Ton*LonB repeatedly interconverts between L- and T-states in concert with ATP hydrolysis cycles.

Structural superposition of the two states reveals that L→T transition is triggered by ATP binding and hydrolysis in the AAA+ module of L-state (L-AAA+ module, Fig. 3A). The ATP-powered vectorial movement of the portal and α/β-subdomains in the L→T transition has been suggested to generate mechanical forces to pull substrate into the hexameric chamber (Cha *et al.*, 2010). It was suggested that the ATP-powered L→T transition of an L-AAA+ module is coupled to the T→L transition of an adjacent T-AAA+ module in the hexamer. Three L-AAA+ and three T-AAA+ modules are alternatively arranged in the hexameric conformation of *Ton*LonB (Cha *et al.*, 2010). A modeling study in which an L-AAA+ module is replaced with a T-AAA+ module revealed a significant clash between adjacent T-AAA+ modules (Cha *et al.*, 2010), indicating that two neighboring AAA+ modules cannot maintain T-state simultaneously in the hexamer. If an L-AAA+ module adjacent to a T-AAA+ module underwent L→T transition, there would be steric clash between the L-AAA+ module undergoing the ATP-powered L→T transition and the adjacent T-AAA+ module. Repulsion energy induced by the steric clash provokes T→L transition of the T-AAA+ module to relieve the clash.

A LonB protease from *Thermococcus kodakarensis* KOD1 (*Tk*LonB) showed ATP-independent proteolytic activity against unfolded protein substrates (Fukui *et al.*, 2002), indicating that the translocation of unfolded proteins to proteolytic sites occurred in the absence of ATP. It was suggested that a large entrance pore of LonB is responsible for the ATP-independent proteolytic activity *Tk*LonB (Fukui *et al.*, 2002). However, the entrance portal in the hexameric structure of *Ton*LonB is too narrow for unfolded protein

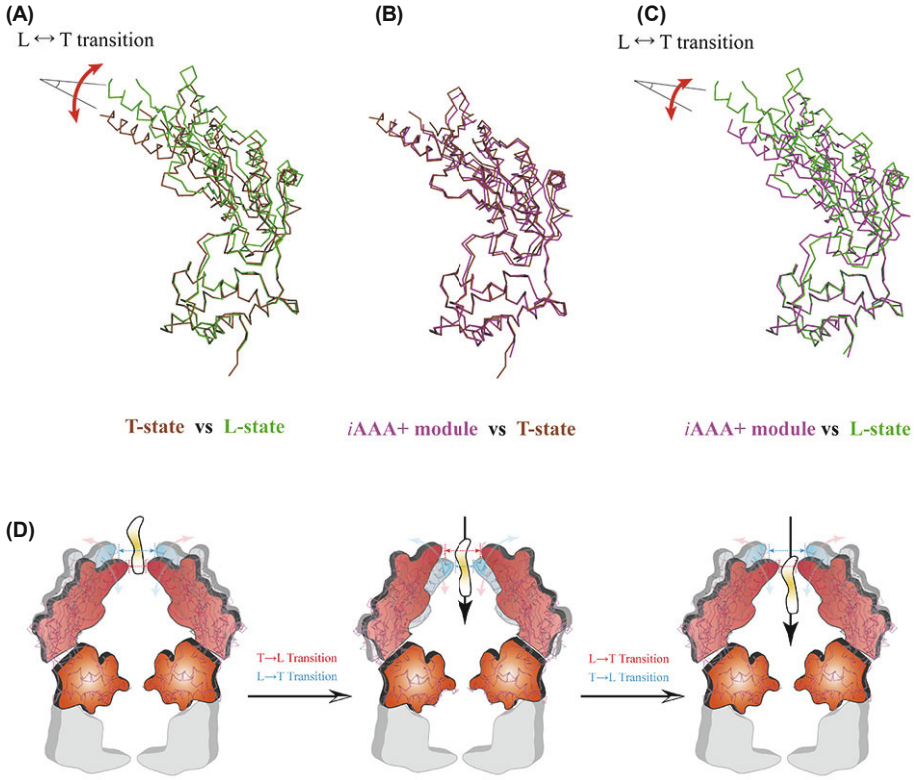


**Fig. 3. Comparison of the AAA+ modules of *Ton*LonB.** (A) Superposition between T-state and L-state of AAA+ modules (PDB code 3K1J). This figure clearly shows the conformational change accompanied by the L↔T transition. (B) Superposition between the *i*AAA+ module and the T-state AAA+ module. (C) Superposition between the *i*AAA+ module and the L-state AAA+ module. The *i*AAA+ module, the T-state AAA+ module, and the L-state AAA+ module are colored in magenta, brown, and green, respectively. (D) Proposed model for the ATP-independent L↔T transition of the AAA+ modules in the hexameric LonB. For clarity, only four AAA+ modules are presented. The protease domain, the α-subdomains, and an unfolded protein substrate are shown as gray, orange, and gradient-yellow, respectively. In the first and third states, T- and L-monomers are shown in red and blue, respectively, whereas T- and L-monomers are shown in blue and red in the second state, respectively.

substrates to pass through (Cha *et al.*, 2010). Structural investigation of the *i*AAA+ module seems to provide explanation for the ATP-independent proteolytic activity. There is no clear electron density for nucleotide at the ATP-binding site in the *i*AAA+ module, indicating that *i*AAA+ would resemble the L-AAA+ module in the hexameric *Ton*LonB structure. However, the conformation of the *i*AAA+ module is virtually identical to the AAA+ module of T-state (Fig. 3B). According to the superposition between the *i*AAA+ module and the T-AAA+ module, the overall Cα RMSD is 0.85 Å and the α/β- and portal subdomains are rotated ~2.33° relative to each other (Fig. 3B). In contrast, the overall Cα RMSD between the *i*AAA+ module and the L-AAA+ module is 1.85 Å, and the α/β- and portal subdomains are rotated ~11.86° relative to each other (Fig. 3C). The superposition between the *i*AAA+ module and the L-AAA+ module indicates that the interconversion of the AAA+ module between L- and T-states could occur in the absence of ATP (Fig. 3C). Consequently, the ATP-independent mechanical motion of the AAA+ modules could guide unfolded protein substrates to proteolytic sites inside the hexameric chamber (Fig. 3D).

### Revising the classification of AAA+ modules of Lon proteases

The AAA+ superfamily has been classified on the basis of sequence homology and structural features (Iyer *et al.*, 2004; Ammelburg *et al.*, 2006; Erzberger and Berger, 2006). Especially, the latest analysis provides a well-defined classification of AAA+ proteins (Erzberger and Berger, 2006). In this classification, AAA+ proteins were divided into seven major clades: Clamp loader clade, Initiator clade, Classic clade, Superfamily III helicase clade, HCLR clade, H2-insert clade, and PS-II insert clade. The replication factor subunit B (RFC-B), a clamp loader clade, has been cited as a prototype of the AAA+ modules (Erzberger and Berger, 2006). The α/β-subdomain of RFC-B is composed of a central five-stranded parallel β-sheet (β5-, β1-, β4-, β3-, and β2 in order) sandwiched by five α-helices (α3, α4, α6, α8, and α10) and four $3_{10}$ helices (α2, α5, α7, and α9). The α-subdomain of RFC-B is composed of a four-helix bundle (α11, α12, α13, and α14) and a $3_{10}$ helix (α1) (Supplementary data Fig. S1). The other six clades are characterized by the differences arising from the insertion of secondary structural elements at defined places within and around the prototypical AAA+ module of RFC-B (Erzberger and Berger, 2006).

According to the previous classifications, Lon proteases belong to the same clade, HslU/ClpX/Lon/ClpAB-C or HCLR clade. It should be noted that structural information on the AAA+ module of Lon proteases was not exploited in the previous classifications. The HCLR clade is characterized by the presence of a β-hairpin insertion between α8 and β4 in the RFC-B AAA+ module, which is referred to as the "Pre-sensor 1 β-hairpin insertion (PS-1 insertion)" (Iyer *et al.*, 2004). The crystal structure of monomeric *Bacillus subtilis* LonA (*Bs*LonA) confirmed the existence of the PS-1 insertion in the AAA+ module of LonA (Fig. 4B) (Duman and Löwe, 2010). However, the structural feature of the *i*AAA+ module of *Ton*LonB is not compatible with the definition of the HCLR clade. The *i*AAA+ module of *Ton*LonB has not only Ins3, which is topologically equivalent to the PS-1 insertion, but also two other insertions: Ins1 and Ins2 (Fig. 4C). Ins2 is topologically identical to a helix 2 insertion (H2

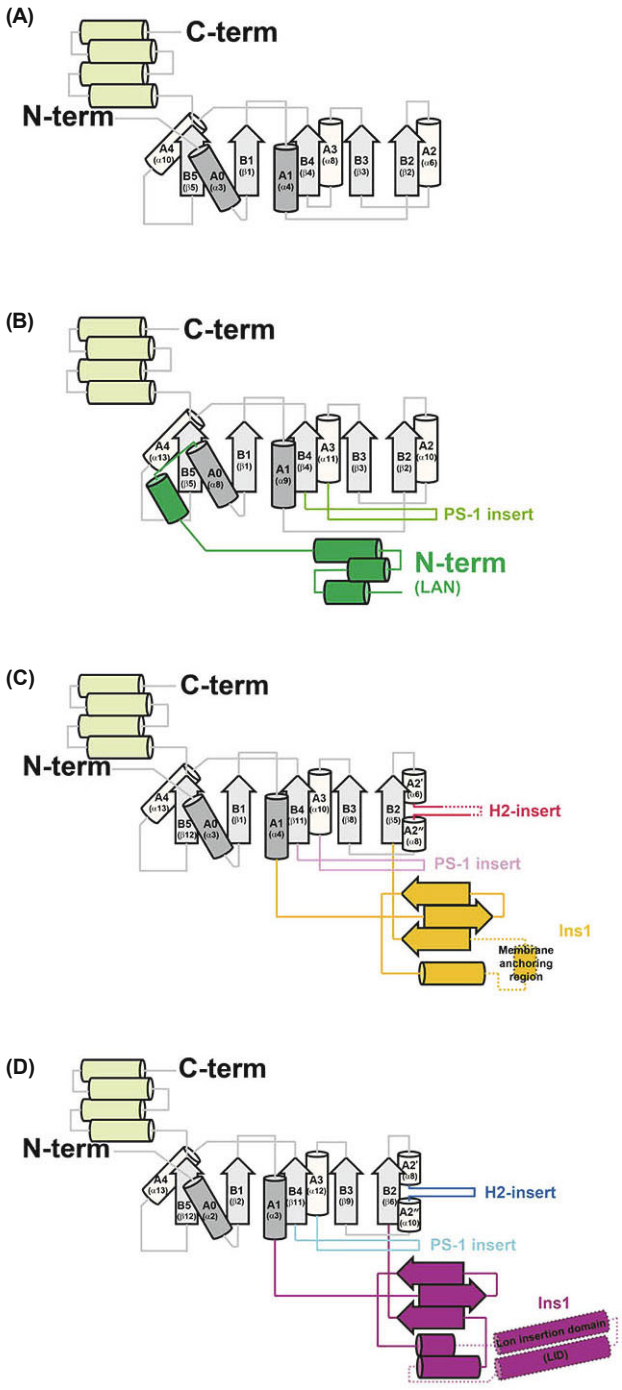


**Fig. 4. Topology diagrams of the AAA+ modules.** The α-subdomain and α/β-subdomain are shown in lime and gray tones, respectively. "A0-A4" and "B1-B5" indicate the standard secondary structure numbering of the AAA+ module, and the secondary structure numberings in parentheses correspond to each specific AAA+ module. (A) Topology diagram of the AAA+ module in RFC-B. (B) Topology diagram of the AAA+ module in *Bs*LonA. PS-1 insert and LAN are shown in yellow-green and forest-green, respectively. (C) Topology diagram of the AAA+ module in *Ton*LonB. PS-1 insert, H2 insert, and Ins1 are shown in light pink, hot pink, and yellow, respectively. Putative membrane-anchoring region and disordered region of H2-insert are presented by dotted lines. (D) Topology diagram of the AAA+ module in the Lon-like protease from *Meiothermus taiwanensis* (PDB code 4FW9). PS-1 insert, H2 insert, and Ins1 are shown cyan, blue, and purple, respectively. The putative LID region is presented by dotted lines.

insertion), a β-hairpin insertion which disrupts α6 in the RFC-B AAA+ module (between α6 and α8 in the *Ton*LonB) (Fig. 4C). The H2-insert clade is characterized by the presence of both the PS-1 insertion and the H2 insertion. In the H2-insert clade, no member has an additional insertion, like Ins1, between α4 and β2 in the RFC-B AAA+ module (Fig. 4C) (Erzberger and Berger, 2006). Therefore, it is not appropriate to classify the AAA+ module of *Ton*LonB as the H2-insert clade. Alternatively, we propose that the AAA+ module of LonB belongs to a new clade, named "H2 & Ins1 insert clade (HINS clade)".

Recently, an ATP-independent Lon-like protease was characterized (Fig. 4D) (Liao *et al.*, 2012). The Lon-like protease forms a symmetrical barrel assembled from six crescent-shaped monomers, each of which is composed of an AAA-like domain and a protease domain (Liao *et al.*, 2013). In AAA+ modules, a glutamate residue in the Walker-B motif (Glu246 in the *Ton*LonB) and an arginine residue in the sensor-2 motif (Arg379 in the *Ton*LonB) are required for ATP hydrolysis (Cha *et al.*, 2010). In the AAA-like domain, however, the two residues are replaced by alanine and valine, respectively, which explains why the AAA-like domain has no ATPase activity but maintains an ability to bind symmetrically six nucleotides per its hexameric chamber (Liao *et al.*, 2012). The AAA-like domain has three insertions: PS-1 insertion, H2-insertion, and Lon insertion domain (LID), which is composed of a three-stranded antiparallel β-sheet and a four-helix bundle between α4 and β2 in the RFC-B AAA+ module (Fig. 4D) (Li *et al.*, 2013). The LID of the Lon-like protease is topologically equivalent to the Ins1 of *i*AAA+ module of *Ton*LonB (Fig. 4C and D), which indicates that the AAA-like domain also belongs to the HINS clade in structural aspect.

## Acknowledgements

We thank the staff of beamline 17A at the Photon factory for help with data collection. This work was supported by the National Research Foundation of Korea Grant (NRF-2015R1A2A2A01004168 and NRF-2015M1A5A1037480) and the KIOST in-house research program (PE99314).

## References

**Adams, P.D., Grosse-Kunstleve, R.W., Hung, L.W., Ioerger, T.R., McCoy, A.J., Moriarty, N.W., Read, R.J., Sacchettini, J.C., Sauter, N.K., and Terwilliger, T.C.** 2002. PHENIX: building new software for automated crystallographic structure determination. *Acta Crystallogr. D Biol. Crystallogr.* **58**, 1948–1954.

**Ammelburg, M., Frickey, T., and Lupas, A.N.** 2006. Classification of AAA+ proteins. *J. Struct. Biol.* **156**, 2–11.

**An, Y.J., Lee, C.R., Supangat, S., Lee, H.S., Lee, J.H., Kang, S.G., and Cha, S.S.** 2010. Crystallization and preliminary X-ray crystallographic analysis of Lon from *Thermococcus onnurineus* NA1. *Acta Crystallogr. Sect. F. Struct. Biol. Cryst. Commun.* **66**, 54–56.

**Cha, S.S., An, Y.J., Lee, C.R., Lee, H.S., Kim, Y.G., Kim, S.J., Kwon, K.K., De Donatis, G.M., Lee, J.H., Maurizi, M.R., *et al.*** 2010. Crystal structure of Lon protease: molecular architecture of gated entry to a sequestered degradation chamber. *EMBO J.* **29**, 3520–3530.

**Collaborative Computational Project, Number 4.** 1994. The CCP4 suite: programs for protein crystallography. *Acta Crystallogr. D Biol. Crystallogr.* **50**, 760–763.

**Duman, R.E. and Löwe, J.** 2010. Crystal structures of *Bacillus subtilis* Lon protease. *J. Mol. Biol.* **401**, 653–670.

**Emsley, P. and Cowtan, K.** 2004. Coot: model-building tools for molecular graphics. *Acta Crystallogr. D Biol. Crystallogr.* **60**, 2126–2132.

**Erzberger, J.P. and Berger, J.M.** 2006. Evolutionary relationships and structural mechanisms of AAA+ proteins. *Annu. Rev. Biophys. Biomol. Struct.* **35**, 93–114.

**Fukui, T., Eguchi, T., Atomi, H., and Imanaka, T.** 2002. A membrane-bound archaeal Lon protease displays ATP-independent proteolytic activity towards unfolded proteins and ATP-dependent activity for folded proteins. *J. Bacteriol.* **184**, 3689–3698.

**Goldberg, A.L. and St John, A.C.** 1976. Intracellular protein degradation in mammalian and bacterial cells: Part 2. *Annu. Rev. Biochem.* **45**, 747–803.

**Gottesman, S.** 1996. Proteases and their targets in *Escherichia coli*. *Annu. Rev. Genet.* **30**, 465–506.

**Gottesman, S.** 2003. Proteolysis in bacterial regulatory circuits. *Annu. Rev. Cell. Dev. Biol.* **19**, 565–587.

**Hershko, A. and Ciechanover, A.** 1992. The ubiquitin system for protein degradation. *Annu. Rev. Biochem.* **61**, 761–807.

**Iyer, L.M., Leipe, D.D., Koonin, E.V., and Aravind, L.** 2004. Evolutionary history and higher order classification of AAA+ ATPases. *J. Struct. Biol.* **146**, 11–31.

**Li, J.K., Liao, J.H., Li, H., Kuo, C.I., Huang, K.F., Yang, L.W., Wu, S.H., and Chang, C.I.** 2013. The N-terminal substrate-recognition domain of a LonC protease exhibits structural and functional similarity to cytosolic chaperones. *Acta Crystallogr. D. Biol. Crystallogr.* **69**, 1789–1797.

**Liao, J.H., Ihara, K., Kuo, C.I., Huang, K.F., Wakatsuki, S., Wu, S.H., and Chang, C.I.** 2013. Structures of an ATP-independent Lon-like protease and its complexes with covalent inhibitors. *Acta Crystallogr. D. Biol. Crystallogr.* **69**, 1395–1402.

**Liao, J.H., Kuo, C.I., Huang, Y.Y., Lin, Y.C., Lin, Y.C., Yang, C.Y., Wu, W.L., Chang, W.H., Liaw, Y.C., Lin, L.H., *et al.*** 2012. A Lon-like protease with no ATP-powered unfolding activity. *PLoS One* **7**, e40226.

**McClellan, A.J., Tam, S., Kaganovich, D., and Frydman, J.** 2005. Protein quality control: chaperones culling corrupt conformations. *Nat. Cell Biol.* **7**, 736–741.

**Otwinowski, Z. and Minor, W.** 1997. Processing of X-ray diffraction data collected in oscillation mode. *Macromolecular Crystallography Pt A* **276**, 307–326.

**Rotanova, T.V., Botos, I., Melnikov, E.E., Rasulova, F., Gustchina, A., Maurizi, M.R., and Wlodawer, A.** 2006. Slicing a protease: structural features of the ATP-dependent Lon proteases gleaned from investigations of isolated domains. *Protein Sci.* **15**, 1815–1828.

**Sauer, R.T. and Baker, T.A.** 2011. AAA+ proteases: ATP-fueled machines of protein destruction. *Annu. Rev. Biochem.* **80**, 587–612.

**Sauer, R.T., Bolon, D.N., Burton, B.M., Burton, R.E., Flynn, J.M., Grant, R.A., Hersch, G.L., Joshi, S.A., Kenniston, J.A., Levchenko, I., *et al.*** 2004. Sculpting the proteome with AAA(+) proteases and disassembly machines. *Cell* **119**, 9–18.

**Talarico, L.A., Gil, M.A., Yomano, L.P., Ingram, L.O., and Maupin-Furlow, J.A.** 2005. Construction and expression of an ethanol production operon in Gram-positive bacteria. *Microbiology* **151**, 4023–4031.